JOC*Article*

Theoretical Investigation of Optical and Electronic Property Modulations of π-Conjugated Polymers Based on the Electron-Rich 3,6-Dimethoxy-fluorene Unit

Li Yang,[†] Ai-Min Ren,[†] Ji-Kang Feng,*[,†,‡] and Ji-Fen Wang[†]

State Key Laboratory of Theoretical and Computational Chemistry, Institute of Theoretical Chemistry and College of Chemistry, Jilin University, Changchun 130023, Jilin University, Changchun 130023

Jikangf@yahoo.com

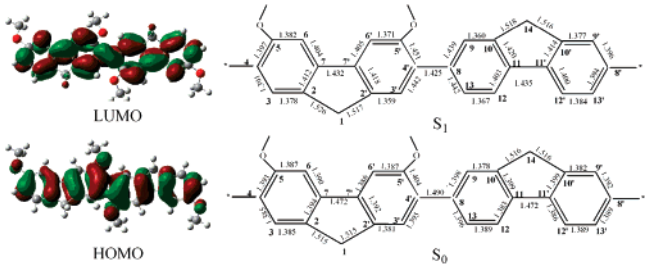

Poly(fluorene)-type materials are widely used in polymer-based emitting devices. One of the drawbacks of light-emitting diodes based on polyfluorene derivatives is the injection of holes from the anode due to the high ionization potential (IP) of most derivatives. Substitution by electron-donating alkoxy substituents or by adding charge carriers on the conjugated polymer's backbone produces a remarkable influence on its electrical and optical properties. In this contribution, we apply quantum-chemical techniques to investigate a family of π-conjugated polymers with substituted dimethoxy groups at the 3,6 positions of the fluorene ring, namely, poly(2,7-(3,6-dimethoxy-fluorene)(PDMOF), poly(2,7-(3,6-dimethoxy-fluorene)-*co*-alt-fluorene (PDMOFF), and poly(2,7-(3,6-dimeth-oxy-fluorene)-*co*-alt-2,5-thiophene (PDMOFT). The electronic properties of the neutral molecules, HOMO−LUMO gaps (Δ_{H-L}), in addition to the positive and negative ions, are studied using the B3LYP functional. The lowest excitation energies (E_g) and the maximal absorption wavelength λ_{abs} of PDMOF, PDMOFF, and PDMOFT are studied by employing time-dependent density functional theory (TD-DFT) and the ZINDO semiempirical method. The IP, EA, and E_g values of each polymer were obtained by extrapolating those of the oligomers to the inverse chain length equal to zero ($^1/_n = 0$). The influence of the presence of methoxy groups on the fluorene moiety on the ionization potential is especially emphasized. The outcomes show that the HOMO energies of these systems under study increase by about 0.4 eV and the IP values decrease by about 0.3 eV compared to those of the corresponding polyfluorene. Both effects result in a reduction of the energy barrier for the injection of holes in related polymeric light-emitting devices and should contribute to the enhancement of their performances. Because of the cooperation with thiophene in PDMOFT, which results in a good planar conformation, both the hole-creating and electron-accepting abilities are improved.

1. Introduction

Conjugated polymers have been the subject of considerable academic and industrial research in recent years because of their possible applications in optoelectronic devices such as field-effect transistors,[1] solar cells,[2] and light-emitting diodes (LED).[3,4] Among these polymers, polyfluorene derivatives show interesting and unique chemical and physical properties because their emission at certain wavelengths spans the entire visible spectrum, they have high fluorescence efficiency, and they possess good thermal stability.[5−10] It is known that an optimized light-emitting diode requires efficient and balanced charge

[†] State Key Laboratory of Theoretical and Computational Chemistry.
[‡] College of Chemistry.

(1) Dimitrakopoulos, C. D.; Malenfant, P. R. L. *Adv. Mater.* **2002**, *14*, 99.
(2) Brabec, C. J.; Sariciftci, N. S.; Hummelen, J. C. *Adv. Funct. Mater.* **2001**, *11*, 15−26.
(3) Kraft, A.; Grimsdale, A. C.; Holmes, A. B. *Angew. Chem., Int. Ed.* **1998**, *37*, 402.
(4) Mitschke, U.; Bäuerle, P. *J. Mater. Chem.* **2000**, *10*, 1471.
(5) Liu, B.; Yu, W.; Lai, Y.; Huang, W. *Chem. Commun.* **2000**, 551.

10.1021/jo0481102 CCC: $30.25
Published on Web 03/10/2005

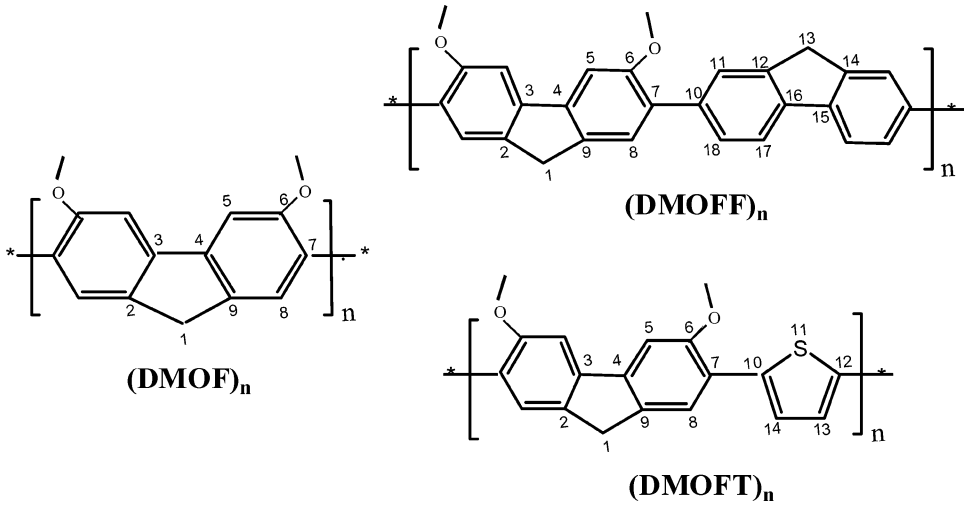

FIGURE 1. Sketch map of the structures.

injection, good and comparable mobilities for both holes and electrons, and a high luminescence quantum yield.[11−14] Nonetheless, one of the drawbacks for light-emitting diodes based on polyfluorene derivatives is the injection of holes from the anode due to the high ionization potential (IP) of most derivatives. The HOMO and LUMO levels and thus the IP and EA values of these π-electron systems can be changed by varying the number of monomer units, introducing electron-donating alkoxy substituents, or modifying the terminal positions of the chains by electron-releasing (donor) and -withdrawing (acceptor) substituents.

However, theoretical studies on the electronic structures of polymers have made great contributions to the rationalization of the properties of known polymers[15−17] and the prediction those of yet unknown polymers.[18−20] Semiempirical methods are known to yield satisfactory geometries and can provide good insight into the electronic structure of large systems. In the present work, we have shown that scaled semiempirical energy gaps are in good agreement with the reported experimental results. Correlation effects can be very important for the study of the electronic structure of molecules and should be taken into account, particularly when one is interested in the evaluation of the energy gap. In this sense, density functional theory (DFT), due to its feature of including the electronic correlation in a computationally efficient manner, can be used in larger molecular systems. In its formalism, the ionization potential and electron affinity are well-defined properties than can be calculated.

Here we studied three series of π-conjugated oligomers and polymers based on the electron-rich 3,6-dimethoxy-fluorene unit, poly(2,7-(3,6-dimethoxy-fluorene) (PDMOF) (1), poly(2,7-(3,6-dimethoxy-fluorene)-*co*-alt-fluorene (PDMOFF) (2), and poly(2,7-(3,6-dimeth-oxy-fluorene)-*co*-alt-2,5-thiophene (PDMOFT) (3)[21] (shown in Figure 1) by using density functional methods and semiempirical models. Then we applied the experimentally well-known[17,22−28] reciprocal rule for polymers, which states that many properties of homopolymers tend to vary linearly as functions of the reciprocal chain length, to investigate the IP, EA, HOMO−LUMO gap (Δ_{H-L}), and lowest excitation energies (E_g).[29−32] A distinct advantage of this approach is that it can provide the convergence behavior of the structural and electronic properties of

(6) Sainova, D.; Miteva, T.; Nothofer, H.; Scherf, U.; Glowacki, I.; Ulanski, J.; Fujikawa, H.; Neher, D. *Appl. Phys. Lett.* **2000**, *76*, 1810.
(7) Weinfurtner, K.; Fujikawa, H.; Tokito, S.; Taga, Y. *Appl. Phys. Lett.* **2000**, *76*, 2502.
(8) Virgili, T.; Lidzey, D. G.; Bradley, D. D. C. *Adv. Mater.* **2000**, *12*, 58.
(9) Bernius, M.; Inbasekaran, M.; O'Brien, J.; Wu, W. *Adv. Mater.* **2000**, *12*, 1737.
(10) Yu, W.; Pei, J.; Cao, Y.; Huang, W.; Heeger, A. *J. Chem. Commun.* **2000**, *76*, 2502.
(11) Oyaizu, K.; Iwasaki, T.; Tsukahara, Y.; Tsuchida, E. *Macromolecules* **2004**, *37*, 1257.
(12) Peng, Q.; Lu, Z. Y.;; Huang, Y.; Xie, M. G.; Han, S. H.; Peng, J. B.; Cao, Y. *Macromolecules* **2004**, *37*, 260.
(13) Yang, R. Q.; Tian, R. Y.; Yang, W.; Cao, Y. *Macromolecules* **2003**, *36*, 7453.
(14) Yang, N. C.; Lee, S. M.; Yoo, Y. M.; Kim, J. K.; Suh, D. H. *J. Polym. Sci., Part A* **2004**, *42*, 1058.
(15) Ma, J.; Li, S. H.; Jiang, Y.-S. *Macromolecules* **2002**, *35*, 1109.
(16) Sheats, J. R.; Antoniadis, H.; Hueschen, M.; Leonard, W.; Niller, H.; Moon, R.; Roitman, D.; Stocking, A. *Science* **1996**, *273*, 884.
(17) Lahti, P. M.; Obrzut, J.; Karasz, F. E. *Macromolecules* **1987**, *20,* 2023.
(18) De Oliveira, M. A.; Duarte, H. A.; Pernaut, J. M.; De Almeida, W. B. *J. Phys. Chem. A* **2002**, *104*, 8256.
(19) *Primary Photoexcitations in Conjugated Polymers: Molecular Exciton Versus Semiconductor Band Model*; Sariciftci, N. S., Ed.; World Scientific: Singapore, 1997.
(20) Janak, J. F. *Phys. Rev. B* **1978**, *18*, 7165.
(21) Beaupré, S.; Leclerc, M. *Macromolecules* **2003**, *36*, 8986.
(22) Winokur, M. J.; Slinker, J.; Huber, D. L. *Phys. Rev. B* **2003**, *67*, 184106.
(23) Donat-bouillud, A.; Lévesque, L.; Tao, Y.; D'Iorio, M.; Beaupré, S.; Blondin, P.; Ranger, M.; Bouchard, J.; Leclerc, M. *Chem. Mater.* **2000**, *12*, 1931−1936.
(24) Zeng, G.; Yu, W. L.; Chua, S. J.; Huang, W. *Macromolecules* **2002**, *35*, 6907−6914.
(25) Lee, S. H.; Nakamura, T.; Tsutsui, T. *Org. Lett.* **2001**, *3*, 2005−2007.
(26) Wong, K. T.; Wang, C. F.; Chou, C. H.; Su, Y. O.; Lee, G. H.; Peng, S. M. *Org. Lett.* **2002**, *4*, 4439−4442.
(27) Ma, J.; Li, S. H.; Jiang, Y.-S. *Macromolecules* **2002**, *35*, 1109−1115.
(28) Klaerner, G.; Miller, R. D. *Macromolecules* **1998**, *31*, 2007−2009.
(29) (a) Ford, W. K.; Duke, C. B.; Salaneck, W. R. *J. Chem. Phys.* **1982**, *77*, 5030. (b) Ford, W. K.; Duke, C. B.; Paton, A. *J. Chem. Phys.* **1982**, *77*, 4564.
(30) Diaz, A. F.; Crowley, J.; Baryon, J.; Gardini, G. P.; Torrance, J. B. *J. Electroanal. Chem.* **1981**, *121*, 355.
(31) Brédas, J. L.; Chance, R. R.; Silbey, R. *Mol. Cryst. Liq. Cryst.* **1981**, *77*, 319.
(32) Brédas, J. L.; Chance, R. R.; Silbey, R. *Phys. Rev. B: Condens. Matter* **1982**, *26*, 5843.

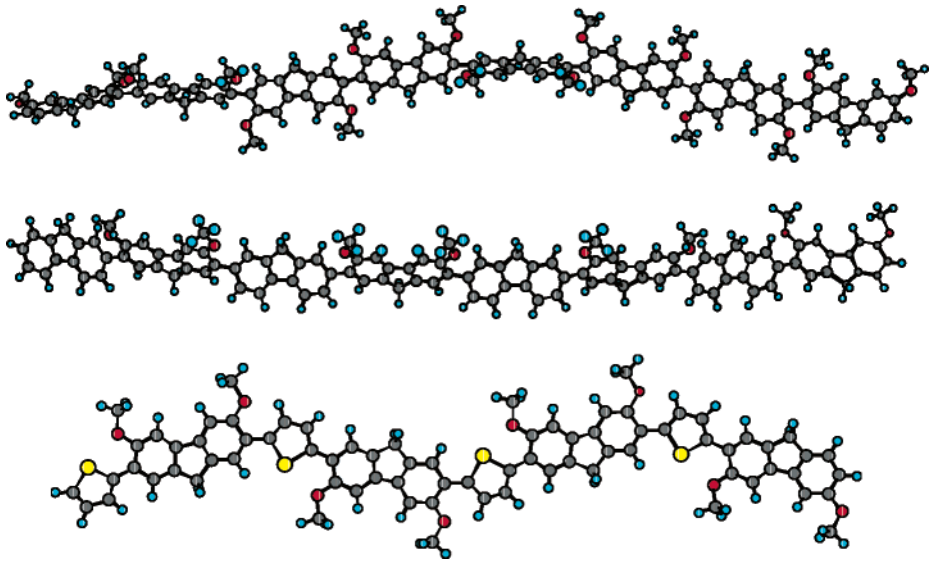

FIGURE 2. Optimized structures for $(DMOF)_8$ (top), $(DMOFF)_4$ (middle), and $(DMOFT)_4$ (bottom).

oligomers. In particular, the influence of the substitution of the fluorene ring with two electron-donating dimethoxy groups on the ionization potential (IP) is the goal of this work.

2. Computational Details

All of the calculations on these oligomers studied in this work have been performed on the SGI origin 2000 server using the Gaussian 03 program package.[33] The energy gap has been estimated in two ways, namely, from the HOMO−LUMO gaps and the lowest excited energies. Calculations of the electronic ground state of oligomers were carried out using density functional theory (DFT), B3LYP/6-31G. The excited geometries were optimized by ab initio CIS/6-31G.[34,35] The transition energies will be calculated at the ground-state and excited-state geometries using ZINDO and TD-DFT/B3LYP calculations, and the results will be compared to the available experimental data. The CI calculations include 196 singly (SCI) excited configurations in the ZINDO method. The nature of the excited states, as well as the positive and negative ions with regard to "electron−hole" creation, is relevant to their use in OLED materials. The various properties of polymers, such as IP, EA, Δ_{H-L}, and E_g, are obtained by employing the reciprocal rule for polymers, which has been successfully employed in investigating several series of polymers.[7,15,29,36−38] The linearity between the calculated properties and the reciprocal chain length is excellent for the homologous series of oligomers.

3. Results Discussion

3.1. Ground-State Structural Properties. The sketch map of the structures is depicted in Figure 1, and the optimized structures by B3LYP/6-31G of $(DMOF)_8$, $(DMOFF)_4$, and $(DMOFT)_4$ are plotted in Figure 2

. The investigated polymers correspond to copolymers P1, P2, and P3 in the literature,[21] and the main difference is that the ones under study substitute 9,9-dihexyl with hydrogen in fluorene rings for the sake of reducing the time of calculation. In fact, it has been proven that the presence of alkyl groups at the 9 positions does not significantly affect the equilibrium geometries and thus does not effect the electronic and optical properties.[39,40] Furthermore, to explore the effect of the addition of two methoxy units at the 3,6 positions on fluorene, our group investigated polyfluorene[36] as a comparison.

The results of the optimized structures for the oligomeric molecules of $(DMOF)_n$ ($n = 1-4$, 6, 8), $(DMOFF)_n$, and $(DMOFT)_n$ ($n = 1-4$)[41] show that the bond lengths and angles do not suffer appreciable variation with the oligomer size in the series of $(DMOF)_n$ as well as $(DMOFF)_n$ and $(DMOFT)_n$. This suggests that we can describe the basic structures of the polymers as their oligomers. Because the dihedral angle between the two phenyl rings in the fluorene segment of all series of oligomers is fixed by ring-bridged atoms, which tend to keep their normal tetrahedral angles in their ring linkage to keep their quasi-planar conformation, the dihedral angles in them are no more than 1°. The largest dihedral

(33) Frisch, M. J.; Trucks, G. W.; Schlegel, H. B.; Scuseria, G. E.; Robb, M. A.; Cheeseman, J. R.; Montgomery, J. A., Jr.; Vreven, T.; Kudin, K. N.; Burant, J. C.; Millam, J. M.; Iyengar, S. S.; Tomasi, J.; Barone, V.; Mennucci, B.; Cossi, M.; Scalmani, G.; Rega, N.; Petersson, G. A.; Nakatsuji, H.; Hada, M.; Ehara, M.; Toyota, K.; Fukuda, R.; Hasegawa, J.; Ishida, M.; Nakajima, T.; Honda, Y.; Kitao, O.; Nakai, H.; Klene, M.; Li, X.; Knox, J. E.; Hratchian, H. P.; Cross, J. B.; Adamo, C.; Jaramillo, J.; Gomperts, R.; Stratmann, R. E.; Yazyev, O.; Austin, A. J.; Cammi, R.; Pomelli, C.; Ochterski, J. W.; Ayala, P. Y.; Morokuma, K.; Voth, G. A.; Salvador, P.; Dannenberg, J. J.; Zakrzewski, V. G.; Dapprich, S.; Daniels, A. D.; Strain, M. C.; Farkas, O.; Malick, D. K.; Rabuck, A. D.; Raghavachari, K.; Foresman, J. B.; Ortiz, J. V.; Cui, Q.; Baboul, A. G.; Clifford, S.; Cioslowski, J.; Stefanov, B. B.; Liu, G.; Liashenko, A.; Piskorz, P.; Komaromi, I.; Martin, R. L.; Fox, D. J.; Keith, T.; Al-Laham, M. A.; Peng, C. Y.; Nanayakkara, A.; Challacombe, M.; Gill, P. M. W.; Johnson, B.; Chen, W.; Wong, M. W.; Gonzalez, C.; Pople, J. A. *Gaussian 03*, revision B.01; Gaussian, Inc.: Pittsburgh, PA, 2003.

(34) Yang, L.; Ren, A. M.; Feng, J. K.; Liu, X. D.; Ma, Y. G.; Zhang, H. X. *Inorg. Chem.* **2004**, *43*, 5961.

(35) Yang, L.; Ren, A. M.; Feng, J. K.; Ma, Y. G.; Zhang, M.; Liu, X. D.; Shen, J. C.; Zhang, H. X. *J. Phys. Chem. A* **2004**, *108*, 6797.

(36) Wang, J. F.; Feng, J. K.; Ren, A. M.; Liu, X. J.; Ma, Y. G.; Lu, P.; Zhang, H. X. *Macromolecules* **2004**, *37*, 3451.

(37) Brébdas, J. L.; Silbey, R.; Boudreaux, D. S.; Chance, R. R. *J. Am. Chem. Soc.* **1983,** *105*, 6555.

(38) Kwon, O.; McKee, M. L. *J. Phys. Chem. A* **2000**, *104*, 7106.

(39) Foresman, J. B.; Head-Gordon, M.; Pople, J. A. *J. Phys. Chem.* **1992**, *96*, 135.

(40) Belletête, M.; Beaypré, S.; Bouchard, J.; Blondin, P.; Leclerc, M.; Durocher, G. *J. Phys. Chem. B* **2000**, *104*, 9118.

(41) The selected optimized bond lengths, bond angles, and dihedral angles are included in Table 1S.

TABLE 1. Dihedral Angles and Inter-ring Distances of $(DMOF)_n$, $(DMOFF)_n$, and $(DMOFT)_n$ ($n = 1-4, 6, 8$) Obtained by DFT//B3LYP/6-31G Calculations

molecule	dihedral angles (deg)	inter-ring distances (Å)	molecule	dihedral angles (deg)	inter-ring distances (Å)	molecule	dihedral angles (deg)	inter-ring distances (Å)
$(DMOF)_n$			$(DMOFF)_n$			$(DMOFT)_n$		
$n = 1$			$n = 1$	40.7	1.488	$n = 1$	18.2	1.465
$n = 2$	50.4	1.489	$n = 2$	40.3	1.488	$n = 2$	16.1	1.462
$n = 3$	50.3	1.489	$n = 3$	40.5	1.487	$n = 3$	16.9	1.462
$n = 4$	50.1	1.489	$n = 4$	40.9	1.488	$n = 4$	16.1	1.462
$n = 6$	50.3	1.489						
$n = 8$	50.4	1.489						

angles are the inter-ring dihedral angles between the two adjacent fluorene units in $(DMOF)_n$ and $(DMOFF)_n$ (Φ (8, 7, 10, 18)) and the angle between the fluorene and thiophene rings in $(DMOFT)_n$ (Φ (8, 7, 10, 14)). The optimized dihedral angles between the subunits of these oligomers are summarized in Table 1in addition to the inter-ring distances. As shown in Table 1, Φ (8, 7, 10, 18) is around 50 and 40° in $(DMOF)_n$ and $(DMOFF)_n$, respectively, which is larger than that in PF (∼36°),[36] indicating that the addition of methoxy groups onto the fluorene moiety at the 3,6 positions increases the steric hindrance and leads to a more twisted conformation. Moreover, Φ (8, 7, 10, 18 (14)) decreases sharply from ∼50 to ∼40 to ∼16° on going from $(DMOF)_n$ to $(DMOFF)_n$ to $(DMOFT)_n$, suggesting a more planar conformation in $(DMOFT)_n$ because of the strong push−pull effect between the fluorene ring and the thiophene ring. It can also be explained by a weak interaction between the methoxy group and the hydrogen atom of the thiophene ring.[21]

3.2. Frontier Molecular Orbitals. It will be useful to examine the highest occupied orbitals and the lowest virtual orbitals for these oligomers and polymers because the relative ordering of the occupied and virtual orbitals provides a reasonable qualitative indication of the excitation properties[42] and the ability of electron or hole transport. Because the first dipole-allowed electron transitions, as well as the strongest electron transitions with the largest oscillator strength, correspond almost exclusively to the promotion of an electron from HOMO to LUMO (see section 3.4), we have plotted the contour plots of the HOMO and LUMO orbitals of $(DMOF)_n$, $(DMOFF)_n$, and $(DMOFT)_n$ ($n = 1-4$, 6, 8) by B3LYP/6-31G in Figure 3.

As shown in Figure 3, all of the frontier orbitals are spread over the whole π-conjugated backbone, although the largest contributions come from the different parts of the chromophores. There is antibonding between the bridge atoms of the inter-ring, and there is bonding between the bridge carbon atom and its conjoint atoms of the intra-ring in the HOMO. On the contrary, there is bonding in the bridge single bond of the inter-ring and antibonding between the bridge atom and its neighbor in the intra-ring in the LUMO. In general, the HOMO possesses antibonding character between the subunits. This may explain the nonplanarity that is observed for these oligomers in their ground states. However, the LUMO of all of the oligomers generally shows bonding character between the two adjacent subunits. This implies that the singlet excited state involving mainly the promotion of an electron from the HOMO to the LUMO should be more planar. In fact, the electronic cloud distributed in the front orbitals of $(DMOF)_n$ is similar to that of $(DMOFF)_n$ and $(DMOFT)_n$.

In the experiment, the HOMO and LUMO energies were calculated from one empirical formula proposed by Brédas et al. that is based on the onset of the oxidation and reduction peaks measured by cyclic voltammetry, assuming that the absolute energy level of ferrocene/ferrocenium is 4.8 eV below vacuum.[43] The HOMO and LUMO energies can be calculated nicely by density functional theory (DFT) in this study. The negative of the HOMO ($-\epsilon_{HOMO}$) and LUMO energies ($-\epsilon_{LUMO}$) of these orbitals in $(DMOF)_n$, $(DMOFF)_n$, and $(DMOFT)_n$ have been compiled in Table 2 together with the experimental data. As shown in Table 2, although there are discrepancies between the calculated values and the observed data, the variation trends are alike.

From Table 2, it can be seen that the HOMO energies are ∼−4.7, ∼−4.8, and ∼−4.5 eV in PDMOF, PDMOFF, and PDMOFT, respectively, which are all higher than the HOMO energy of PF (∼−5.1 eV),[36] indicating that the presence of 3,6-dimethoxy groups have significantly improved the hole-creating properties of the copolymers. Furthermore, the HOMO energies in PDMOFT are higher than those in PDMOF and PDMOFF, suggesting that cooperation with thiophene further contributes to the enhancement of its hole-injection performance resulting from the more planar conformation. The LUMO energies slightly change in PDMOF (−1.1 eV) and PDMOFF (−1.3 eV) compared to that in PF (−1.3 eV),[36] suggesting that the electron-accepting ability does not worsen with the introduction of 3,6-dimethoxy groups. It is noteworthy that the LUMO energies in PDMOFT (−1.7 eV) sharply decrease about 0.4 eV more than those in PF. This is reasonable because the HOMO shows inter-ring antibonding character and the LUMO shows inter-ring bonding character, so the variation of torsional angles should have a larger effect on the LUMO. Indeed, the decrease in the dihedral angles induced by the presence of the thiophene moiety should enhance the bonding character between the two subunits and thus stabilize the LUMO. It is obvious that PDMOFT is either a good hole-creating or electron-accepting material.

3.3. HOMO−LUMO Gaps and the Lowest Excitation Energies. In theory, the energy gap of the polymer $(M)_n$ is the orbital energy difference between the highest occupied molecular orbital (HOMO) and the lowest unoc-

(42) De Oliveira, M. A.; Duarte, H. A.; Pernaut, J.-M.; De Almeida, W. B. *J. Phys. Chem. A* **2000**, *104*, 8256−8262.

(43) Morisaki, Y.; Ishida, T.; Chujo, Y. *Polym. J.* **2003**, *35*, 501−506.

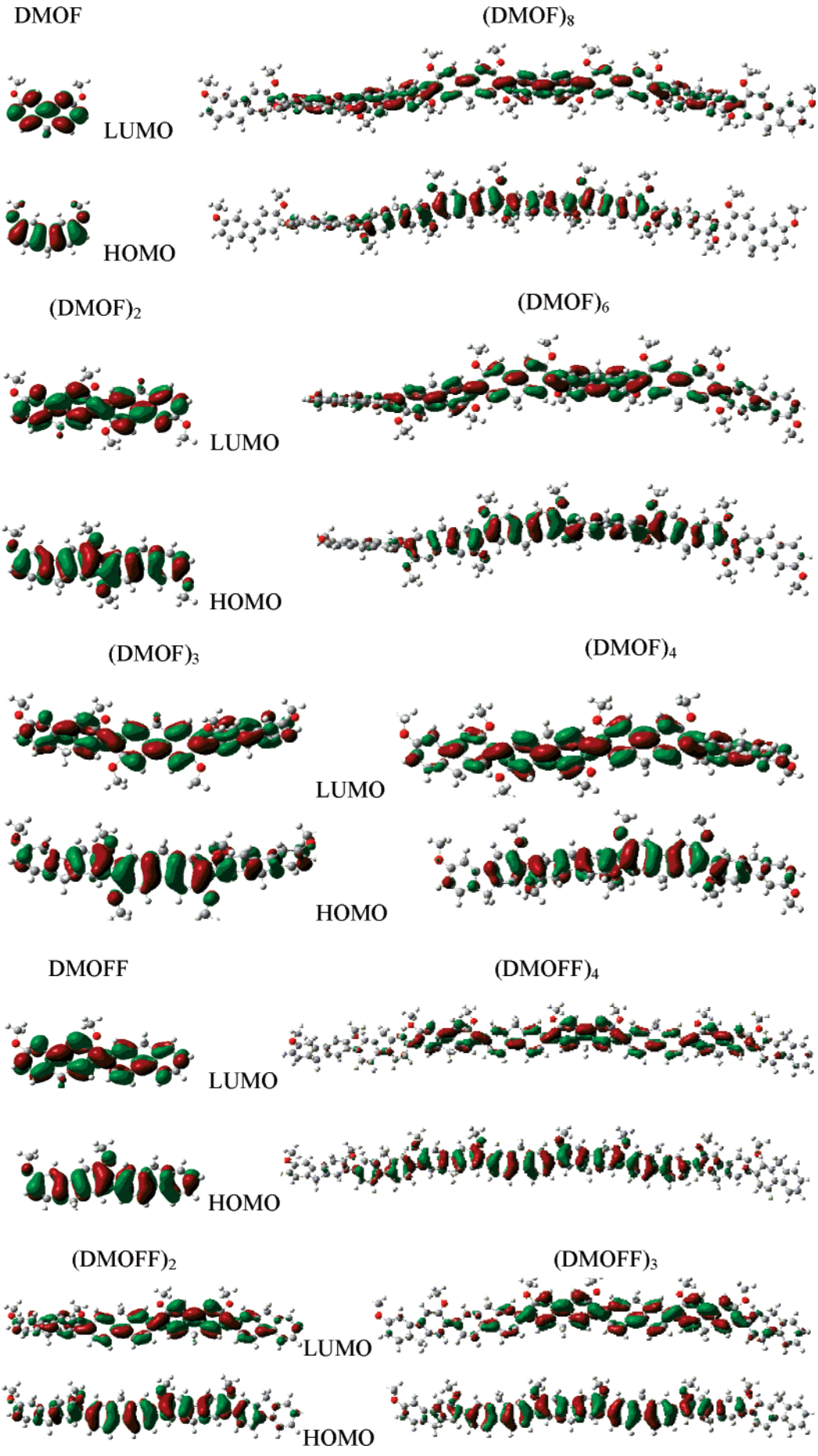
DMOF
(DMOF)8
LUMO
HOMO
(DMOF)2
(DMOF)6
LUMO
HOMO
(DMOF)3
(DMOF)4
LUMO
HOMO
DMOFF
(DMOFF)4
LUMO
HOMO
(DMOFF)2
(DMOFF)3
LUMO
HOMO

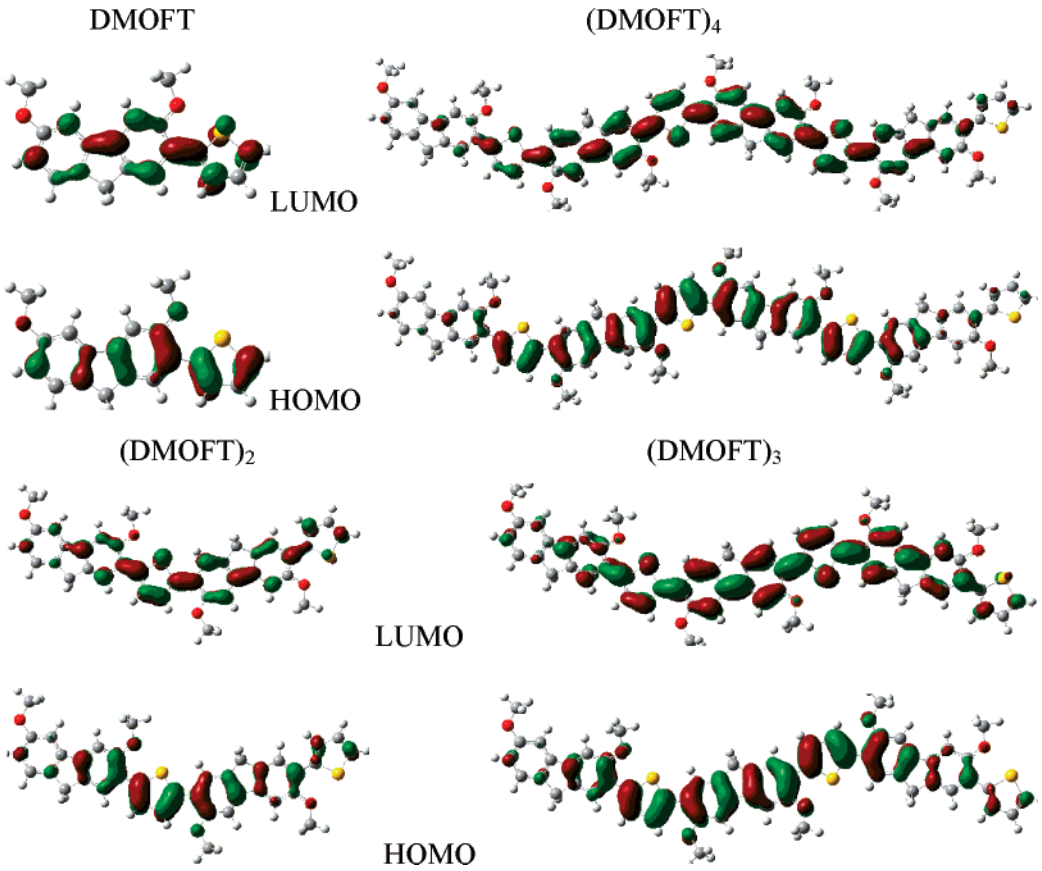

FIGURE 3. HOMO and LUMO orbitals of $(DMOF)_n$, $(DMOFF)_n$, and $(DMOFT)_n$ (n = 1−4, 6, 8) by B3LYP/6-31G.

TABLE 2. Negative of the HOMO ($-\epsilon_{HOMO}$) and LUMO Energies ($-\epsilon_{LUMO}$) (eV) of the Oligomers in $(DMOF)_n$, $(DMOFF)_n$, and $(DMOFT)_n$

oligomer	$-\epsilon_{HOMO}$	$-\epsilon_{LUMO}$	oligomer	$-\epsilon_{HOMO}$	$-\epsilon_{LUMO}$	oligomer	$-\epsilon_{HOMO}$	$-\epsilon_{LUMO}$
$(DMOF)_n$			$(DMOFF)_n$			$(DMOFT)_n$		
$n = 1$	5.47	0.75	$n = 1$	5.19	1.09	$n = 1$	5.17	1.25
$n = 2$	5.04	0.98	$n = 2$	4.95	1.27	$n = 2$	4.69	1.61
$n = 3$	4.87	1.05	$n = 3$	4.88	1.31	$n = 3$	4.56	1.70
$n = 4$	4.78	1.08	$n = 4$	4.85	1.33	$n = 4$	4.50	1.75
$n = 6$	4.70	1.10	exptl	5.67	2.30	exptl	5.21	2.53
$n = 8$	4.67	1.10						
exptl	5.65	2.38						

cupied molecular orbital (LUMO)[44−46] when $n = \infty$. Our HOMO−LUMO gaps (Δ_{H-L}) are obtained from density functional theory (DFT) calculations. The experimental energy gap is the lowest transition (or excitation) energy from the ground state to the first dipole-allowed excited state and thus should be abbreviated E_g (S), with the meaning obtained from spectra. Considering the experimental data, the energy gap from the differences of the orbital energies between the HOMO and LUMO is crude. The implicit assumption underlying this approximation is that the lowest singlet excited state can be described by only one singly excited configuration in which an electron is promoted from the HOMO to the LUMO. In addition, the orbital energy difference between the HOMO and the LUMO is still an approximate estimate to the transition energy because the transition energy also contains significant contributions from some two-electron integrals. The real situation in the experiment is that an accurate description of the lowest singlet excited state requires a linear combination of a number of excited configurations, although the one mentioned above often plays a dominant role. To directly compare the experimental band gap with the theoretical data in quantity, we obtained more rigorous information on the nature of the lowest singlet excited state by the ZINDO semiempirical method and by employing time-dependent DFT (TD-DFT) calculations, which have been used to study systems of increasing complexity because of their relatively low computational cost and also to include the electron correlation effects in its formalism.

Here, the HOMO−LUMO gaps and lowest singlet excited energies of all of the oligomers in PDMOF, PDMOFF, and PDMOFT are listed in Table 3. The

(44) Hay, P. J. *J. Phys. Chem. A* **2002**, *106*, 1634−1641.
(45) Curioni, A.; Andreoni W.; Treusch, R.; Himpsel, F. J.; Haskal, E.; Seidler, P.; Heske, C.; Kakar, S.; van Buuren, T.; Terminello, L. J. *Appl. Phys. Lett.* **1998**, *72*, 1575−1577.
(46) Hong, S. Y.; Kim, D. Y.; Kim, C. Y.; Hoffmann, R. *Macromolecules* **2001**, *34*, 6474−6481.

TABLE 3. HOMO−LUMO Gaps (eV) by DFT and the Lowest Excitation Energies (eV) by TDDFT and ZINDO in Oligomers of $(DMOF)_n$, $(DMOFF)_n$, and $(DMOFT)_n$

oligomer	Δ_{H-L}	E_g(TD)	E_g(ZIN)	oligomer	Δ_{H-L}	E_g(TD)	E_g(ZIN)	oligomer	Δ_{H-L}	E_g(TD)	E_g(ZIN)
$(DMOFF)_n$				$(DMOFF)_n$				$(DMOFT)_n$			
$n = 1$	4.72	4.33	4.02	$n = 1$	4.10	3.80	3.74	$n = 1$	3.92	3.77	3.53
$n = 2$	4.06	3.72	3.86	$n = 2$	3.68	3.29	3.57	$n = 2$	3.08	2.93	2.95
$n = 3$	3.82	3.44	3.66	$n = 3$	3.57	3.25	3.55	$n = 3$	2.86	2.62	2.81
$n = 4$	3.70	3.28	3.56	$n = 4$	3.52	3.24	3.53	$n = 4$	2.75	2.48	2.77
$n = 6$	3.60	3.26	3.54	$\boldsymbol{n = \infty}$	**3.32**	**2.99**	**3.46**	$\boldsymbol{n = \infty}$	**2.35**	**2.02**	**2.47**
$n = 8$	3.57	3.23	3.46	exptl	3.37[a]			exptl	2.68[a]		
$\boldsymbol{n = \infty}$	**3.40**	**3.02**	**3.44**								
exptl	3.27[a]										

[a] Reference 21.

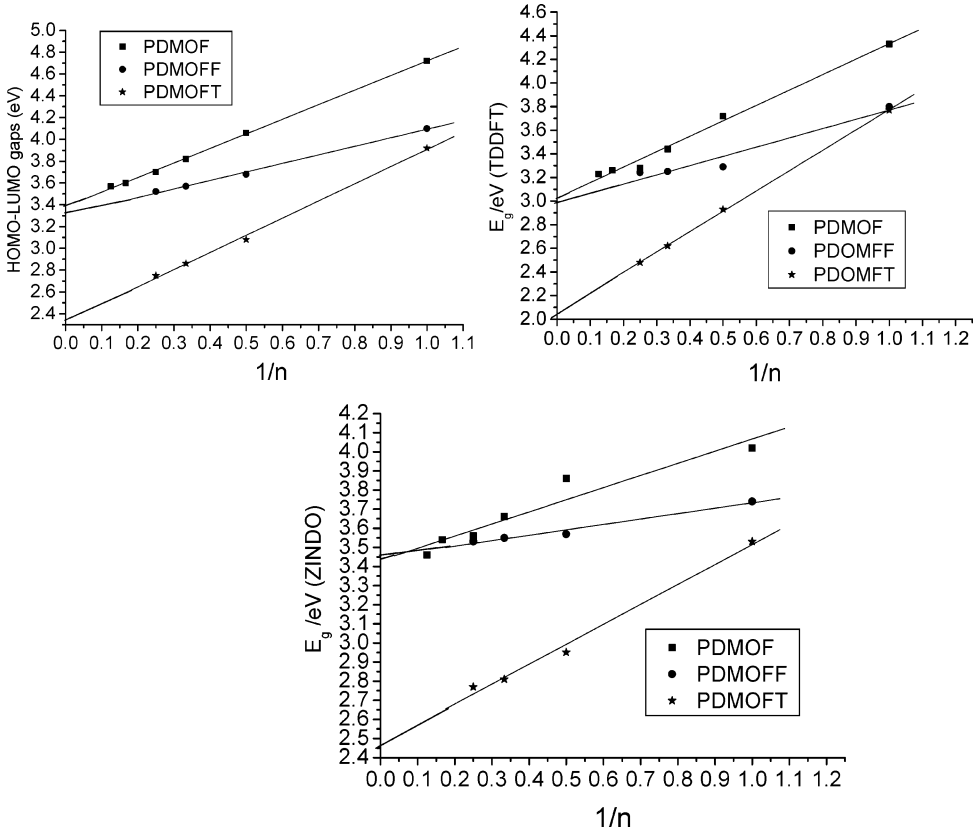

FIGURE 4. HOMO−LUMO gaps (Δ_{H-L}) by B3LYP and the lowest excitation energies E_g (S) by ZINDO and TD-DFT as a function of reciprocal chain length n in oligomers of $(DMOF)_n$, $(DMOFF)_n$, and $(DMOFT)_n$.

relationships between the calculated Δ_{H-L} and the E_g (S) and the inverse chain length are plotted in Figure 4. There is a good linear relation between the energy gaps by two methods and the inverse chain length. Indeed, as shown in Table 3, the B3LYP/6-31G HOMO−LUMO energy gaps (Δ_{H-L}) are found to be higher than the TDDFT// B3LYP/6-31G energies of the corresponding HOMO−LUMO transitions. Because the energy of the vertical electronic transition from a doubly occupied MO to a vacant MO is predicted to be smaller than their energy gap, it must be ascribed to the reduced interelectronic interaction upon the single one-electron excitation. (The interaction can be conceptually interpreted in a simple way as the balance between coulomb and exchange terms, and we expect that it should decrease progressively with increasing size of the π-conjugated system.)[47]

Interestingly, in this paper the Δ_{H-L} and E_g (ZIN) presented in Table 3 yield better agreement with the experimental data than the E_g (TD) in all series. (Namely, the discrepancies between the experimental data are 0.13, 0.05, and 0.33 eV for Δ_{H-L} and 0.17, 0.09, and 0.21 eV for E_g (ZIN) for PDMOF, PDMOFF, and PDMOFT, respectively.) The energetic positions of E_g (TD) from our results in all of the copolymers are higher than the experimental value from the edge of the electronic band (namely, 0.25, 0.38, and 0.66 eV between E_g (TD) and the experimental data for PDMOF, PDMOFF, and PDMOFT, respectively), and this goes along with the increase in conjugation lengths; this discrepancy is in part due to the relatively large size of the studied systems and the reciprocal dependence of the energy gap on the

(47) Brière, J. F.; Côté, M. *J. Phys. Chem. B* **2004**, *108*, 3123.

number of repeat units usually observed in organic systems. Additionally, it should be borne in mind that solid-state effects (such as polarization effects and intermolecular packing forces) have been neglected in the calculations.[48,49]

At the same time, it is also necessary to check the validity of the excitation energies that were calculated by TD-DFT. The excitation energies calculated by TD-DFT with the current exchange-correlation functions are not reliable when the calculated excitation energies are higher than the negative of the HOMO energies.[15,36] Combining Tables 2 and 3, we can show that in all cases the TD-DFT excitation energies are below the negative of the HOMO energies and thus may be numerically reliable. For the copolymers studied in this work, neither the HOMO−LUMO gap approach nor the TDDFT or ZINDO excitation energies provide reasonably good results.

In all cases, the band gaps extrapolated by the lowest excitation energies (E_g (S)) and the HOMO−LUMO gaps (Δ_{H-L}) have basically the same trend to meet the experimental data. By comparing the calculated values of PF with the results of our series copolymer, we can find the influence of electron-donating methoxy on fluorene. The band gaps obtained by HOMO−LUMO gaps, TD-DFT, and ZINDO in PDMOF and PDMOFF are all higher than those in PF (3.33, 2.91, and 3.18 eV, respectively, with the same corresponding methods),[36] ascribed to the breaking conjugation backbone by the presence of the electron-donating methoxy groups. Alternatively, because of the low LUMO energy resulting from a more planar conformation, as mentioned above, the energy gap is reduced sharply in PDMOFT. By all accounts, the results of each method indicate the same conclusion: the increase in conjugation in the backbone narrowed its band gap and vice versa.

In addition, the effective conjugation length (ECL) can be estimated from the calculations of a series of oligomers. For polymers, the ECL is a highly important variable in determining electron properties such as band gaps, absorption coefficients, emission quantum yields, and so forth.[15,50] The ECL can be explained as the minimum number of repeating units necessary to produce saturation of a physical property (e.g., absorption or emission maxima). We take 0.01 eV as the convergence threshold of the excitation energies with the chain length based on the obtained linearity between the excitation energy and reciprocal chain length.[51] Therefore, the ECL of PDMOF is estimated to be around 8 units by TDDFT. For PDMOFF and PDMOFT, shorter ECL values of about 4 and 5 units, respectively, are estimated by TD-DFT. By ZINDO, they are 11, 5, and 7 units for PDMOF, PDMOFF, and PDMOFT, respectively. Both methods produce the same result: PDMOFF and PDMOFT have a shorter effective conjugation length than PDMOF because the dramatically twisted segments in the structure of PDMOF block the conjugated backbone.

TABLE 4. Ionization Potentials, Electron Affinities, and Extraction Potentials for Each Molecule (in eV)[a]

eV	IP(v)	IP(a)	HEP	EA(v)	EA(a)	EEP
			$(DMOF)_n$			
$n = 1$	7.05	6.91	6.78	−0.86	−0.68	−0.49
$n = 2$	6.22	6.07	5.92	−0.19	−0.006	0.17
$n = 3$	5.84	5.72	5.59	0.09	0.24	0.38
$n = 4$	5.62	5.52	5.41	0.26	0.38	0.54
$n = 6$	5.37	5.30	5.23	0.46	0.54	0.62
$n = 8$	5.23	5.17	5.12	0.53	0.64	0.74
$\boldsymbol{n = \infty}$	**5.08**	**5.01**	**4.92**	**0.60**	**0.78**	**0.88**
			$(DMOFF)_n$			
$n = 1$	6.41	6.27	6.14	0.12	0.07	0.24
$n = 2$	5.81	5.72	5.63	0.41	0.54	0.65
$n = 3$	5.58	5.50	5.43	0.63	0.73	0.81
$n = 4$	5.42	5.37	5.32	0.78	0.84	0.91
$\boldsymbol{n = \infty}$	**5.14**	**5.10**	**5.08**	**0.91**	**1.07**	**1.10**
			$(DMOFT)_n$			
$n = 1$	6.56	6.39	6.25	0.14	0.03	0.15
$n = 2$	5.72	5.57	5.45	0.61	0.74	0.86
$n = 3$	5.38	5.27	5.18	0.90	1.00	1.09
$n = 4$	5.20	5.10	5.03	1.06	1.17	1.22
$\boldsymbol{n = \infty}$	**4.80**	**4.71**	**4.66**	**1.29**	**1.50**	**1.58**

[a] The suffixes (v) and (a) indicate vertical and adiabatic values, respectively.

3.4. Ionization Potentials and Electron Affinities. As mentioned in the Introduction, efficient injection and transport of both holes and electrons are important parameters in the rational design of optimized light-emitting diodes. Ionization potentials (IP) and electron affinities (EA) are used to estimate the energy barrier for the injection of both holes and electrons into the polymer. Table 4contains the ionization potentials (IP), electron affinities (EA), both vertical (v, at the geometry of the neutral molecule) and adiabatic (a, optimized structure for both the neutral and charged molecule), and extraction potentials (HEP and EEP for the hole and electron, respectively) that refer to the geometry of the ions.[52,53]

In all cases in Table 4, the energies required to create a hole in the polymer are ∼5.0, 5.1, and 4.7 eV, whereas the extraction of an electron from the anion requires ∼0.8, ∼1.0, and ∼1.4 eV for $(DMOF)_n$, $(DMOFF)_n$, and $(DMOFT)_n$, respectively. The measured values of IP and EA for corresponding P1 and P3 are 5.65 and 2.38 and 5.21 and 2.53 eV, respectively,[21] which differed within 1 eV for both IP(a) and EA(a) from our calculated values of 5.08 and 0.78 and 4.71 and 1.50 eV.

To appreciate the influence of the substitution of the fluorene ring with two electron-donating methoxy groups on the ionization potential (IP), we will compare PDMOF and PDMOFT to similar copolymers reported in the literature (PDOF and PFT) that are not bearing a methoxy group at the 3,6 positions. Janietz et al.[54] have reported values of the ionization potential and the electron affinity (EA) for 2,7-(9,9-dihexylfluorene) (PDOF)

(48) Puschning, P.; Ambrosch-Draxl, C.; Heimel, G.; Zojer, E.; Resel, R.; Leising, G.; Kriechbaum, M.; Graupner, W. *Synth. Met*. **2001**, *116*, 327.
(49) Eaton, V. J.; Steele, D. *J. Chem. Soc., Faraday Trans. 2* **1973**, *2*, 1601.
(50) Burrows, P. E.; Shen, Z.; Bulovic, V.; McCarty, D. M.; Forrest, S. R.; Cronin, J. A.; Thompson, M. E. *J. Appl. Phys.* **1996**, *79*, 7991−8006.
(51) Charas, A.; Barbagallo, N.; Morgado, J.; Alcacer, L. *Synth. Met*. **2001**, *122*, 23.
(52) Curioni, A.; Boero, M.; Andreoni, W. *Chem. Phys. Lett*. **1998**, *294*, 263.
(53) Wang, I.; Estelle, B. A.; Olivier, S.; Alain, I.; Baldeck, P. L. *J. Opt. A: Pure Appl. Opt*. **2002**, *4*, S258.
(54) Janietz, S.; Bradley, D. D. C.; Grell, M.; Giebeler, C.; Inbasekaran, M.; Woo, E. P. *Appl. Phys. Lett*. **1998**, *73*, 2453.

TABLE 5. Electronic Transition Data Obtained by TDDFT and ZINDO Methods for $(DMOF)_n$ (n = 1−4, 6, 8) at the B3LYP/6-31G Optimized Geometry

electronic transitions	TDDFT//B3LYP/6-31G			ZINDO		transition dipole moment (D)		
	λ_{abs} (nm)	×c4	main configurations	λ_{abs} (nm)	×c4	*X*	*Y*	*Z*
			DMOF					
$S_0 \rightarrow S_1$	286.43	0.27	HOMO → LUMO(0.62)	308.7	0.29	4.36	0.00	0.00
$S_0 \rightarrow S_2$	272.47	0.03	HOMO-1 → LUMO(0.64)	305.7	0.02	−1.09	0.00	0.00
$S_0 \rightarrow S_3$	254.55	0.05	HOMO-2 → LUMO(0.56)	267.9	0.22	3.56	0.00	0.00
			HOMO → LUMO+2(0.33)					
			$(DMOF)_2$					
$S_0 \rightarrow S_1$	333.46	1.04	HOMO → LUMO(0.66)	321.6	1.60	−10.40	0.85	0.00
$S_0 \rightarrow S_2$	296.05	0.00	HOMO → LUMO+1(0.57)	279.7	0.02	0.00	0.00	1.08
			HOMO-1 → LUMO(0.35)					
$S_0 \rightarrow S_3$	288.62	0.00	HOMO-1 → LUMO(0.44)	261.9	0.37	−0.40	4.55	−0.01
			HOMO → LUMO+1(0.41)					
			$(DMOF)_3$					
$S_0 \rightarrow S_1$	360.56	0.20	HOMO → LUMO(0.64)	348.0	1.95	12.00	0.00	0.46
$S_0 \rightarrow S_2$	322.04	0.00	HOMO → LUMO+1(0.52)	322.3	0.04	0.00	1.62	0.00
			HOMO-1 → LUMO(0.47)					
$S_0 \rightarrow S_3$	317.62	0.01	HOMO → LUMO+1(0.45)	313.4	0.00	0.00	−0.21	0.00
			HOMO-1 → LUMO(0.41)					
			$(DMOF)_4$					
$S_0 \rightarrow S_1$	377.89	0.26	HOMO → LUMO(0.64)	350.1	2.30	−14.82	−0.42	−0.23
$S_0 \rightarrow S_2$	341.34	0.01	HOMO → LUMO+1(0.53)	323.6	0.08	0.11	−1.58	−1.73
			HOMO-1 → LUMO(0.35)					
$S_0 \rightarrow S_3$	336.69	0.00	HOMO-1 → LUMO(0.57)	304.9	0.17	−2.84	0.88	−1.42
			HOMO → LUMO+1(0.39)					
			$(DMOF)_6$					
$S_0 \rightarrow S_1$	380.36	3.43	HOMO → LUMO(0.65)	350.3	4.48	18.26	0.04	0.29
$S_0 \rightarrow S_2$	357.50	0.07	HOMO → LUMO+1(0.50)	333.4	0.09	−0.34	2.52	−0.13
			HOMO-1 → LUMO(0.43)					
$S_0 \rightarrow S_3$	346.39	0.00	HOMO-1 → LUMO(0.51)	315.2	0.52	−5.53	−1.84	0.84
			HOMO → LUMO+1(0.45)					
			$(DMOF)_8$					
$S_0 \rightarrow S_1$	383.97	4.74	HOMO → LUMO(0.61)	351.6	5.76	20.73	−0.03	0.06
$S_0 \rightarrow S_2$	368.99	0.07	HOMO → LUMO+1(0.46)	340.6	0.12	0.32	2.89	−0.03
			HOMO-1 → LUMO(0.45)					
$S_0 \rightarrow S_3$	352.40	0.57	HOMO-1 → LUMO(0.46)	327.0	0.53	5.91	−1.08	0.72
exptl	374[a]	366[b]	HOMO → LUMO+1(0.33)					

[a] The data are measured in solution. [b] The data are measured in film in ref 21.

with IP = 5.80 eV and EA = 2.12 eV. Charas et al.[55] have reported values of IP and EA for PFT with IP = 5.49 and EA= 2.84 eV. Our calculated IP values for PDMOF and PDMOFT are lower than those of similar copolymers PDOF and PFT by about 0.5 eV.

Furthermore, we also compare the calculated results of polyfluorene (PF)[36] to our results of the three series of polymers. It is reported that the IP for PF is 5.39 eV,[36] which is higher than that of all of our copolymers. It is clear from these results that the 3,6-dimethoxy groups allow the modulation of the ionization potentials and make them decrease and thus result in the reduction of the energy barrier to create holes. This should be useful in enhancing the injection of holes from the anode in light-emitting diodes and should be in accord with the analysis from the energies of the HOMOs.

As far as EAs are concerned, EA(a) is 1.24 eV in PF,[36] which is higher than that in PDMOF (0.78 eV) and PDMOFF (1.07 eV) but 0.26 eV lower than that in PDMOFT (1.50 eV), which is similar to the expectation of the energies of the LUMOs that the ability to accept electrons is better in PF than in PDMOF and PDMOFF, whereas an improvement of electron-accepting ability is obtained in PDMOFT. The same calculations are also used to estimate the self-trapping energies of positive and negative charges in the material. Indeed, the traps that characterize the electron transport in the material were identified as the states in which the injected electron is self-trapped in the individual molecules as a consequence of structural relaxation.[50] The correct energy in our scheme is the energy gain of the excess electron due to structural relaxation (i.e., the difference of EA(a) − EA(v), which we also report in Table 4 as the "small-polaron" stabilization energy (SPE) for the electron). The outcomes show that PDMOFT appears to trap the electron more efficiently with a value of 0.21 than PDMOFF and PDMOF with results of 0.16 and 0.18 eV, respectively.

3.5. Absorption Spectra. TDDFT//B3LYP/6-31G and ZINDO have been used on the basis of the optimized geometry to obtain the nature and energy of the singlet−singlet electronic transitions of all of the oligomers in all series under study. Here, we list the transition energies, oscillator strengths, configurations, and transition dipole moments obtained by TDDFT and ZINDO calculations for the most relevant first three singlet excited states in each oligomer of $(DMOF)_n$, $(DMOFF)_n$, and $(DMOFT)_n$ in Tables5−7. As shown in Tables 5−7, all of the electronic transitions are of the $\pi\pi^*$ type and involve both subunits

(55) Charas, A.; Barbagallo, N.; Morgado, J.; Alcacer, L.; *Synth. Met.* **2001**, *122*, 23.

TABLE 6. Electronic Transition Data Obtained by TDDFT and ZINDO Methods for $(DMOFF)_n$ ($n = 1-4$) at the B3LYP/6-31G Optimized Geometry

electronic transitions	TDDFT//B3LYP/6-31G			ZINDO		transition dipole moment (D)		
	λ_{abs} (nm)	×c4	main configurations	λ_{abs} (nm)	×c4	*X*	*Y*	*Z*
			DMOFF					
$S_0 \rightarrow S_1$	326.30	1.16	HOMO → LUMO(0.65)	331.2	1.13	−8.91	−0.29	0.08
$S_0 \rightarrow S_2$	288.44	0.01	HOMO-1 → LUMO(0.59)	309.2	0.13	2.69	0.98	−0.19
			HOMO → LUMO+1(0.33)					
$S_0 \rightarrow S_3$	283.12	0.04	HOMO-2 → LUMO(0.61)	299.5	0.03	1.28	0.19	0.39
			$(DMOFF)_2$					
$S_0 \rightarrow S_1$	377.18	2.60	HOMO → LUMO(0.67)	347.5	3.14	−15.22	0.09	−0.46
$S_0 \rightarrow S_2$	335.17	0.03	HOMO-1 → LUMO(0.55)	319.3	0.10	−2.08	−0.80	1.39
			HOMO → LUMO+1(0.36)					
$S_0 \rightarrow S_3$	334.85	0.04	HOMO → LUMO+1 (0.57)	302.3	0.09	1.93	−1.33	0.45
			HOMO-1 → LUMO (0.40)					
			$(DMOFF)_3$					
$S_0 \rightarrow S_1$	381.98	3.55	HOMO → LUMO(0.66)	349.0	4.55	−18.35	−0.34	0.14
$S_0 \rightarrow S_2$	353.60	0.24	HOMO → LUMO+1(0.53)	330.9	0.38	0.29	−5.00	1.39
			HOMO-1 → LUMO(0.40)					
$S_0 \rightarrow S_3$	351.12	0.04	HOMO-1 → LUMO(0.54)	312.0	0.33	4.65	−0.49	0.55
			HOMO → LUMO+1(0.41)					
			$(DMOFF)_4$					
$S_0 \rightarrow S_1$	382.41	4.57	HOMO → LUMO(0.66)	351.5	5.65	−20.53	0.52	0.05
$S_0 \rightarrow S_2$	363.74	0.52	HOMO → LUMO+1(0.48)	339.3	0.81	−0.46	−7.63	−0.38
			HOMO-1 → LUMO(0.46)					
$S_0 \rightarrow S_3$	354.28	0.03	HOMO-1 → LUMO(0.49)	324.8	0.32	4.67	−0.44	0.20
			HOMO → LUMO+1(0.47)					
exptl	388[a]	380[b]						

[a] The data are measured in solution. [b] The data are measured in film in ref 21.

TABLE 7. Electronic Transition Data Obtained by TDDFT and ZINDO Methods for $((DMOFT)_n$ ($n = 1-4$) at B3LYP/6-31G Optimized Geometry

electronic transitions	TDDFT//B3LYP/6-31G			ZINDO		transition dipole moment (D)		
	λ_{abs} (nm)	×c4	main configurations	λ_{abs} (nm)	×c4	*X*	*Y*	*Z*
			DMOFT					
$S_0 \rightarrow S_1$	328.63	0.82	HOMO → LUMO(0.62)	351.1	0.93	8.29	−0.60	0.10
$S_0 \rightarrow S_2$	293.84	0.03	HOMO-1 → LUMO(0.63)	314.8	0.14	−2.97	−0.85	−0.06
$S_0 \rightarrow S_3$	282.60	0.08	HOMO-2 → LUMO(0.49)	300.1	0.09	−2.06	1.17	0.07
			HOMO → LUMO+2(0.31)					
			$(DMOFT)_2$					
$S_0 \rightarrow S_1$	423.50	2.03	HOMO → LUMO(0.64)	420.0	2.05	13.51	0.47	0.12
$S_0 \rightarrow S_2$	370.02	0.01	HOMO → LUMO+1(0.51)	347.1	0.40	−1.10	−5.26	−0.50
			HOMO-1 → LUMO(0.48)					
$S_0 \rightarrow S_3$	328.76	0.18	HOMO-1 → LUMO(0.42)	328.1	0.01	−0.82	−0.22	0.23
			HOMO → LUMO+1(0.37)					
			$(DMOFT)_3$					
$S_0 \rightarrow S_1$	473.88	2.89	HOMO → LUMO(0.66)	440.9	3.16	−17.21	0.29	−0.04
$S_0 \rightarrow S_2$	420.84	0.01	HOMO → LUMO+1(0.50)	391.4	0.08	0.56	2.05	−1.35
			HOMO-1 → LUMO(0.49)					
$S_0 \rightarrow S_3$	391.06	0.04	HOMO → LUMO+1(0.45)	343.1	0.85	4.63	6.39	0.54
			HOMO-1 → LUMO(0.44)					
			$(DMOFT)_4$					
$S_0 \rightarrow S_1$	500.74	3.99	HOMO → LUMO(0.66)	446.9	4.20	−19.97	0.352	−0.17
$S_0 \rightarrow S_2$	441.28	0.01	HOMO → LUMO+1(0.53)	409.9	0.08	−0.54	0.09	2.53
			HOMO-1 → LUMO(0.46)					
$S_0 \rightarrow S_3$	436.87	0.06	HOMO-1 → LUMO(0.50)	375.2	0.43	−5.18	−2.70	−0.08
exptl	444[a]	446[b]	HOMO → LUMO+1(0.42)					

[a] The data are measured in solution. [b] The data are measured in film in ref 21.

of the molecule. In other words, no localized electronic transitions are calculated among the first three singlet−singlet transitions. Both methods show that excitation to the S_1 state corresponds almost exclusively to the promotion of an electron from the HOMO to the LUMO. The oscillator strength (×c4) and the transition dipole moment along the long axis of the molecule (χ) of the $S_0 \rightarrow S_1$ electronic transition are large in each oligomer. Considering the fact that the oscillator strength is proportional to the square of the transition moment, it is reasonable that the $S_0 \rightarrow S_1$ transition shows a large ×c4 value. Furthermore, the oscillator strength coupling the lowest CT $\pi-\pi^*$ singlet excited state to the ground state increases strongly when going from an isolated molecule to a molecular group. The oscillator strength associated with the S_1 state increases by about 1 order

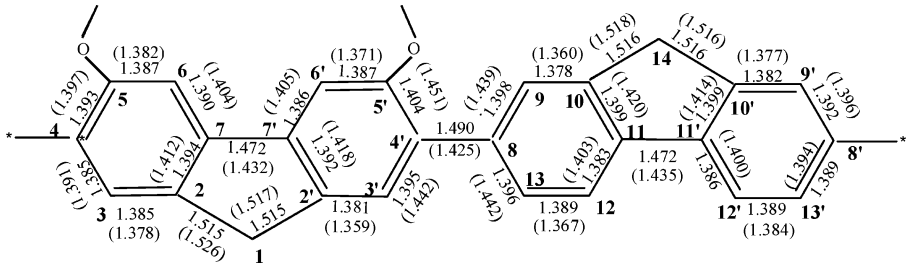

FIGURE 5. Comparison of the lowest excited structure by CIS/6-31g (in parentheses) to the ground structure by HF/6-31g (S_0) of DMOFF.

of magnitude upon adding one repeated unit to the monomers in all series.

Obviously, the strongest absorption peaks are assigned to $\pi\pi^*$ electronic transition character arising exclusively from the $S_0 \rightarrow S_1$ electronic transition composed mainly of the HOMO → LUMO transition. In fact, there is similar character and similar variation trends in $(DMOF)_n$ and $(DMOFT)_n$, as in the cases of $(DMOFF)_n$. We can find in Tables 5−7 that with the conjugation lengths increasing the absorption wavelengths increase progressively, as in the case of the oscillator strengths of the $S_0 \rightarrow S_1$ electronic transition. This is reasonable because the HOMO → LUMO transition is predominant in the $S_0 \rightarrow S_1$ electronic transition and, as the analysis above shows, with the extension of molecular size, the HOMO−LUMO gaps decrease. Because the first allowed transitions are also the absorption maxima, they have the same variation trend, which we would not say more than is needed.

From Tables 5−7, we also find that our values from TDDFT calculations overestimate the absorption spectra compared to the ZINDO results and the experimental data. Many investigations show that TDDFT is a good tool for predicting the absorption spectra of molecules. However, this method has defects when studying extended systems. Frequently, the optical properties reach saturation quickly for short chain lengths, whereas the orbital energies continue to change for longer oligomers. It is known that the exchange-correlation (XC) functionals must decrease with increasing chain length. (This trend of variation is in line with the expectation that in more extended systems the electronic repulsion is smaller.[56,57]) However, because the atomic structures of the molecules are alike and are calculated with the same methods and basis sets, the results can still reflect some variation trend.

3.6. Properties of Excited Structures and the Emission Spectra. It is well known that until now the standard for calculating excited-state equilibrium properties of larger molecules is the configuration interaction singles (CIS) method. However, because of the neglect of electron correlation, CIS results are not accurate enough in many applications. In this study, we hope to investigate the excited-state properties by this method despite the fact that they may not be accurate. Because the calculation of excited-state properties typically requires significantly more computational effort than is needed for the ground states and is dramatically constrained by the size of the molecules, we optimize only the monomers for PDMOFF and PDMOFT and the dimer for PDMOF in view of the molecular weights by CIS/6-31G and compared to their ground structures by HF/6-31G. For the sake of comparison, only DMOFF is plotted in Figure 5. Interestingly, the main characteristics of the frontier orbitals by HF/6-31G are the same as those by B3LYP/6-31G. As shown, some of the bond lengths lengthened but some shortened. We can predict the differences in the bond lengths between the ground (S_0) and lowest singlet excited state (S_1) from MO nodal patterns. Because the lowest singlet state corresponds to an excitation from the HOMO to the LUMO in all of the considered oligomers, we explore the bond-length variation by analyzing the HOMO and LUMO. By comparing Figure 5 with Figure 3, we can see that the HOMO has nodes across the r(2,3), r(7,7′), r(5′,6′), r(2′,3′), r(4′,8), r(12,13), r(9,10), r(9′,10′), and r(11′,11) bonds in DMOFF, but the LUMO is bonding in these regions. Therefore, one would expect a contraction of these bonds; the data in the Figure shows that these bonds are in fact considerably shorter in the excited state. However, the bond length will increase when the bonding changes to antibonding. This can be seen from bond lengths r(4,5), r(2′,7′), r(6′,7′), r(3′,4′), r(6,7), r(2,7), r(4′,5′), r(8,9), r(8,13), r(10,11), r(11,12), r(10′,11′), r(13′,8′), and r(11′,12′) in DMOFF increasing in the excitation compared to those in the the ground state. The data confirm the anticipated elongation of these bonds.

The bridge bonds between two conjugated segments rotate to some extent. The dihedral angle between the two adjacent fluorene units shortened from 50.9 to 21.2° in PDMOFF. In fact, the variations of the structural parameters in PDMOF and PDMOFT are similar to those in PDMOFF. The dihedral angles between the two adjacent fluorene rings in PDMOF and those between the fluorene and thiophene rings in PDMOFT decreased from 50.2 to 26.3° and from 21.7 to nearly 0°, respectively. It is obvious that the excited structure has a strong coplanar tendency in both series; that is, the conjugation is better in the excited structure. For DMOFF, the dihedral angles are no larger than 5° in the excited state. And the dihedral angles in DMOFT are nearly zero after being excited. This indicates that there is a better coplanar conformation for the conjugated backbone in PDMOFT. The smaller band gap and the longer wavelength in the spectra of PDMOFT result from this structural character to a certainty.

For the excited geometries optimized by ab intio CIS, the emission wavelengths are computed by ZINDO and TD-DFT, and the results are compared to the experimental data. As in the case of the absorption spectra,

(56) Grimme, S.; Parac, M. *ChemPhysChem* **2003**, *3*, 292.
(57) Ortiz, R. P.; Delgado, M. C. R.; Casado, J.; Hernández, V.; Kim, O. K.; Woo, H. Y.; Navarrete, L. L. *J. Am. Chem. Soc.* **2004**, *126*, 13363.

both methods reflect that on going from $(DMOF)_2$ to DMOFF and DMOFT the λ_{emi} exhibit bathochromic to long wavelengths, 376.5 < 382.1 < 396.5 nm (ZINDO) and 358.63 < 365.75 < 368.97 nm (TDDFT). This red shift can be attributed to a stronger push−pull effect between the fluorene ring and the thiophene ring, and it may also be explained by a more planar conformation of the ground state of $(DMOFT)_n$. Similar to the absorption spectra, the emission peaks with the strongest oscillator strengths are assigned to $\pi\pi^*$ character arising from the HOMO to LUMO transition in all three copolymers.

4. Conclusions

The oligomers of PDMOF and PDMOFF show more twisted structures compared to those of pristine polyfluorene by the addition of dimethoxy units, whereas because of cooperation with the thiophene rings, PDMOFT exhibits a more planar conformation. All of the decisive molecular orbitals are delocalized on both subunits of the oligomers. The HOMO possesses antibonding character between subunits, which may explain the nonplanarity that is observed for these oligomers in their ground state. However, the LUMO shows bonding character between the two adjacent rings, in agreement with the more planar S_1 excited state. Importantly, the substitution by methoxy groups at the 3,6 positions of the fluorene ring resulted in increased HOMO energies; consequently, the hole injection was greatly improved. Excitation to the S_1 state corresponds almost exclusively to the promotion of an electron from the HOMO to the LUMO. Accordingly, the energy of the $S_0 \rightarrow S_1$ electronic transition follows the HOMO−LUMO energy gap of each oligomer. The first electronic transition gives rise to large values of the oscillator strength in each oligomer. The absorption and emission spectra of $(DMOF)_n$ and $(DMOFF)_n$ appear blue-shifted with the addition of methoxy groups compared to those of PF ascribed to the breaking of the conjugation backbone. On the contrary, they appear bathochromic in $(DMOFF)_n$ compared to those of PF by cooperation with the thiophene ring, which results in better conformations.

Finally, the good agreement between the theoretical results and the experimental data seems to indicate that a rational design of the tunable light-emitting fluorene derivatives and related polymers is possible and should then contribute to the development of organic light-emitting diodes.

Acknowledgment. This work is supported by the Major State Basis Research Development Program (no. 2002CB 613406), the National Nature Science Foundation of China (no. 90101026), and the Key Laboratory for Supramolecular Structure and Material of Jillin University.

Supporting Information Available: Optimized structures and coordinates of the structures. This material is available free of charge via the Internet at http://pubs.acs.org.

JO0481102